Published online 7 December 2010

Nucleic Acids Research, 2011, Vol. 39, No. 5 ***e30***
doi:10.1093/nar/gkq1258

Directed adenovirus evolution using engineered mutator viral polymerases

Taco G. Uil[1], Jort Vellinga[1], Jeroen de Vrij[1], Sanne K. van den Hengel[1], Martijn J. W. E. Rabelink[1], Steve J. Cramer[1], Julia J. M. Eekels[1], Yavuz Ariyurek[2], Michiel van Galen[2] and Rob C. Hoeben[1,*]

[1]Department of Molecular Cell Biology and [2]Human and Clinical Genetics & Leiden Genome Technology Center, Leiden University Medical Center, Leiden, 2300 RC, The Netherlands

Received September 1, 2010; Accepted November 20, 2010

ABSTRACT

Adenoviruses (Ads) are the most frequently used viruses for oncolytic and gene therapy purposes. Most Ad-based vectors have been generated through rational design. Although this led to significant vector improvements, it is often hampered by an insufficient understanding of Ad's intricate functions and interactions. Here, to evade this issue, we adopted a novel, mutator Ad polymerase-based, 'accelerated-evolution' approach that can serve as general method to generate or optimize adenoviral vectors. First, we site specifically substituted Ad polymerase residues located in either the nucleotide binding pocket or the exonuclease domain. This yielded several polymerase mutants that, while fully supportive of viral replication, increased Ad's intrinsic mutation rate. Mutator activities of these mutants were revealed by performing deep sequencing on pools of replicated viruses. The strongest identified mutators carried replacements of residues implicated in ssDNA binding at the exonuclease active site. Next, we exploited these mutators to generate the genetic diversity required for directed Ad evolution. Using this new forward genetics approach, we isolated viral mutants with improved cytolytic activity. These mutants revealed a common mutation in a splice acceptor site preceding the gene for the adenovirus death protein (ADP). Accordingly, the isolated viruses showed high and untimely expression of ADP, correlating with a severe deregulation of E3 transcript splicing.

INTRODUCTION

Viruses with life cycles involving lytic disruption of host cells are being explored for their use as oncolytic agents (1). Oncolytic viruses are unique anticancer agents owing to their ability to amplify their cell-lytic effect through replication and viral spread. This ability, combined with the promise of tumor selectiveness (2), fosters the hope that 'oncolytic virotherapy' could ultimately be more efficient and cause less side effects than existing therapies.

Adenovirus (Ad) is one of the most-studied viruses for oncolytic virotherapy and its potential has been demonstrated by promising preclinical studies and clinical trials (2,3). So far, however, the clinical efficacy of Ad-based virotherapy has not been spectacular; only if viral treatment was combined with more conventional therapies were the results unequivocally positive (4,5). Therefore, many seek to develop improved oncolytic Ads endowed with enhanced tumor cell killing abilities (2,3,6–11). In this regard, in addition to strategies based on rational design, 'bioselection'- or 'directed evolution'-type processes—i.e. methods based on genetic diversification and phenotypic selection—have proven useful to generate new oncolytic Ads (12–15). In studies that took such approaches, whole-genome genetic diversification was achieved either by chemical mutagens, by ultraviolet radiation or by recombination among co-infected Ad serotypes.

Here, we describe the development and validation of a new directed Ad evolution approach that is based on the high mutation rates achieved by engineered mutator Ad polymerases. This 'accelerated evolution' approach is distinct, conceptually and practically, from classical procedures employing chemical or physical mutagens. First, the use of mutator viral polymerases avoids the direct virus inactivating effects normally associated with

*To whom correspondence should be addressed. Tel: +31 71526 9241; Fax: +31 71526 8270; Email: r.c.hoeben@lumc.nl
Present addresses:
Jort Vellinga, Crucell B.V., Leiden, 2301 CA, The Netherlands.
Jeroen de Vrij, Department of Neurosurgery, Erasmus University Medical Center, Rotterdam, 3015 GD, The Netherlands.
Julia J. M. Eekels, Laboratory of Experimental Virology, Department of Medical Microbiology, Academic Medical Center, University of Amsterdam, Amsterdam, 1105 AZ, The Netherlands.

mutagens (i.e. damage to the virus particle and irresolvable DNA lesions) (16,17). Second, and relatedly, our approach is inherently capable of bringing about genetic diversity over repeated viral infection rounds. Importantly, this property allows for multistep viral adaptation processes to occur, i.e. a virus may successively acquire multiple beneficial mutations. Thus, owing to the above aspects, this Ad engineering approach resembles not so much the classical genetic screens, but rather the adaptation processes by which the rapidly mutating RNA viruses—and their recombinant derivatives—can be readily altered or optimized (18–28). In this regard, many such RNA virus adaptation procedures have already led to potency-enhanced oncolytic viruses and/or optimized recombinant vectors.

First, to set up this system, we modified the Ad-encoded polymerase (Ad pol), a protein-primed family B DNA polymerase with proofreading function (29,30). Any mutator activities of the new Ad pol mutants were revealed by a deep-sequencing strategy allowing direct assessment of mutational buildups in replicated viruses. Then, to validate our approach, several of the identified mutator polymerases were used in a directed evolution scheme aimed at increasing Ad's oncolytic potency. Interestingly, this procedure isolated viruses with a common mutation causing untimely expression—due to altered splicing—of the ADP (31,32).

Thus, our data demonstrate that mutator mutants of a viral DNA polymerase can serve to provide the genetic diversity needed for efficient directed evolution of a normally genetically very stable DNA virus. The methodology outlined in our study may represent a general strategy to generate or optimize Ad-based gene delivery vehicles and oncolytic vectors.

MATERIALS AND METHODS

Cell culture

HAdV-5 E1-transformed human embryonic retinoblast cell line 911 and human untransformed diploid foreskin fibroblast cell line VH10 were described previously (33,34). Human ovarian (SKOV-3), breast (SKBR-3) and prostate (PC-3) adenocarcinoma cell lines were obtained from American Type Culture Collection (ATCC). All cell lines were grown at 37°C in DMEM (Gibco BRL, Breda, The Netherlands) supplemented with 8% fetal bovine serum (Gibco BRL) in a humidified atmosphere with 5% CO_2. Cells transduced with lentivirus LV.PP were grown in the presence of 0.7 μg/ml puromycin (MP Biomedicals, Amsterdam, The Netherlands). Cells stably transduced with lentiviruses were named after their parental constituents. For example, an SKOV-3 cell population transduced with lentivirus LV.PP is designated as SKOV-3.PP.

Lentiviral vectors

All lentivirus (LV) plasmids were based on pRRL-cPPT-CMV-X-PRE-SIN (35) or its derivative pLV.CMV.IRES.PURO (36), the latter of which carries an internal ribosomal entry site (IRES) followed by a puromycin resistance gene. LV vectors generated for this study were LV.AdPol, LV.PP and LV.pol-HA, which respectively encode for Ad5 pol, Ad5 pol bicistronically with puromycin and 'pol-HA', a C-terminally HA-tagged version of Ad5 pol. Furthermore, we developed a panel of 23 LV vectors, each encoding a single amino acid substitution mutant of pol-HA. Lentivirus stocks were titrated using a HIV-1 p24 antigen enzyme-linked immunosorbent assay kit (ZeptoMetrix Corp., New York, NY, USA). For the rationale for selecting the Ad pol residues to be mutated, and for further details on vector generation, see Supplementary Data.

Lentivirus-mediated expression of Ad pol variants

Cells seeded in 3-cm wells and grown, in one day, to a confluency of 50–70% were lentivirally transduced overnight in a 2-ml volume in the presence of 8 μg/ml polybrene. Transductions with LV.AdPol, LV.pol-HA and LVs encoding the Ad pol mutants were performed at 50 ng/ml p24 for 911 cells and 150 ng/ml p24 for SKOV-3 cells. Transductions with LV.PP were at 50 ng/ml p24 for SKOV-3 and VH10 cells and at 200 ng/ml p24 for SKBR-3 and PC-3 cells. For immunofluorescence detection of Ad pol variants' expression in transduced cell populations, cells were grown on glass coverslips, fixed and permeabilized with methanol, probed successively with an anti-HA tag and a fluorescien isothiocyanate (FITC)-conjugated antibody, and mounted in Dabco-glycerol for viewing under a fluorescence microscope.

Ad vectors

Two polymerase-defective Ad vectors, AdGLΔPOL (E1- and E3-deleted; reporter genes in place of E1) and HAdV-5ΔPOL (wildtype in sequence apart from the polymerase gene-affecting deletion), were generated as described in Supplementary Data. Viruses were purified by centrifugation on CsCl gradients by standard protocols. The physical viral particle titers (VP/ml) were determined using the fluorescent dye PicoGreen as described by Murakami and McCaman (37).

Ad pol *trans*-complementation assays

For all assays, semiconfluent parallel cultures of 911 cells stably expressing Ad pol variants were incubated with AdGLΔPOL at a multiplicity of infection (MOI) of 0.15 pfu/cell for 1.5–3.5 h. For assays with luciferase-based readout, the infected cells were lysed in lysis mix [25 mM Tris-phosphate (pH 7.8), 2 mM CDTA, 2 mM DTT, 10% glycerol and 1% Triton-X in PBS] and stored at −80°C until luciferase activities were measured (Luciferase Assay System, Promega). See Supplementary Data for the initial setup of the complementation system.

Mutation-accumulation procedure

AdGLΔPOL was subjected to 10 serial viral passages on semiconfluent cultures of 911 cells expressing Ad pol variants. For the first passage, the infections were

carried out in 24-well plate wells at 0.15 pfu/cell. All subsequent passages were performed in six-well plate wells using 300, 30 and 3 µl of the harvested previous infection for inoculation. At 3 or 4 days after each inoculation, those wells were harvested where virtually all cells had been infected—as judged from green fluorescent protein (GFP) expression on day 2—and for which the cytopathic effect (CPE) had become abundant. Harvested infections, consisting of dislodged cells and medium, were freeze-thawed and cleared by centrifugation before being used as inocula for the next passage. To test for any polymerase-proficient recombinants within the virus populations, we performed PCRs on the polymerase region and screened for replication ability on non-complementing cells (i.e. 911 cells). Although one of the initial AdGLΔPOL stocks tested positive for a minute subpopulation of recombinants, all the passaged virus populations—intermediate and final—were negative.

Preparation of viral pools containing approximately 50 clones each

Two different approaches were taken to prepare 50-clone virus pools from the passaged virus populations of the mutation-accumulation experiment. The first approach entailed infection of 911.pol-HA cells in duplicate at 100, 50 and 25 pfu/well in a six-well plate. Of the duplicate sets of infections, one served as an intra-experiment plaque assay titration and was therefore overlaid with 0.5% agarose (Invitrogen) medium. From the other set, the infection containing nearest to 50 clones (as inferred from the intra-experiment titration) was harvested—by collecting cells and medium—at full CPE (day 14). The second, presumably more accurate approach to obtain near 50-clone pools involved the pooling of 50 mostly single-clone infections. For this approach, multiple 96-well plates—seeded with 911.pol-HA cells—were infected with such an MOI that the majority (i.e. about 80%) of the wells were non-infected. The contents of 50 randomly selected infection-positive wells were harvested—after the occurrence of full CPE—and pooled together. In this procedure, the observed fraction of wells found to be infection-negative allowed for the calculation—using the Poisson distribution—of the average number of clones in an infection-positive well. Multiplication of this average clone number with 50 (i.e. the number of pooled infections) gave an approximation of the total number of clones in the pooled population.

Massively parallel sequencing and data analysis

(Procedures for the pilot massively parallel sequencing (MPS) run performed on the spiked test sample can be found in Supplementary Data.) From each 50-clone virus pool obtained in the mutation-accumulation experiment, a 6.5-kb fragment was PCR amplified by Phusion DNA polymerase (Finnzymes/NEB), purified and size selected using the SureClean PCR cleanup kit (Bioline) and, after electrophoresis, the JetSorb gel extraction kit (Genomed) (see Supplementary Data for primer sequences). For each purified product, 100 ng was fragmented by nebulization according to Illumina's 'Preparing Samples for Sequencing Genomic DNA' document. Fragment libraries—size selected for fragments of 200–300 bp—were subsequently prepared using Illumina's 'Preparing Samples for ChiP Sequencing of DNA' document. The libraries were subjected to 32 cycles of single-end sequencing by an Illumina Genome Analyzer II (GAII) instrument using one flowcell lane per sample. Image analysis and base calling were performed by Illumina's Genome Analyzer pipeline (GAPipeline) using default parameters. Sequence reads passing the default Illumina chastity filter (threshold = 0.6) were outputted—by the GERALD module of the GAPipeline—in read files of the SCARF format. These files served—after their conversion to a suitable format—as input for the short read analysis pipeline SHORE (http://1001genomes.org/downloads/shore.html) (38). SHORE carried out alignments [through invocation of GenomeMapper (39)], performed quality filtering (i.e. masking of bases with assigned quality values below a set threshold) and generated forward and reverse consensus summaries (i.e. base counts per position in the reference sequence). Details on the workflow and parameter settings used can be found in Supplementary Data. MPS was also employed to obtain the complete sequences of several individual Ad genomes. Briefly, an Illumina multiplexed sequencing run was performed in one GAII flow cell, after which the resulting data sets were analyzed using the ELAND aligner of the GAPipeline and the Velvet algorithm for *de novo* assembly (http://www.ebi.ac.uk/~zerbino/velvet/) (40).

Directed evolution procedure

HAdV-5ΔPOL was subjected to 10 serial passages on SKOV-3 cells expressing the Ad pol variants and then successively to 10 such rounds on SKOV-3.pol-HA cells. The passaging procedure was as described for the mutation-accumulation procedure except for the following distinctions. First, each infection was harvested by collection of only culture medium (i.e. without cells). Second, harvesting took place at the first sign of CPE, which was mostly at day 3. Third, the MOIs of the successive infections were strived to be kept relatively low. The latter was sought to be achieved by choosing, for each passage, a suitable narrow range of inoculation doses (e.g. 36, 12 and 4 µl of the harvested media of the previous passage) and by subsequently harvesting from among the resultant infections one exhibiting only a modest level of CPE. Virus stocks and passaged populations of HAdV-5ΔPOL all tested negative for any polymerase-proficient recombinants (see mutation-accumulation procedure above).

Cell killing assays

For cytotoxicity assays, semiconfluent cell cultures grown in 96-well plates were infected at the indicated MOIs. The infections were performed in duplicate (pools) or in triplicate (clones). Cell viabilities were measured on day 6 (911.pol-HA) or between days 10 and 15 (SKOV-3.pol-HA, SKOV-3.PP, SKBR-3.PP, PC-3.PP and VH10.PP) using the WST-1 reagent

(Roche). For plaque size assays, semiconfluent SKOV-3.pol-HA cell cultures in six-well plates were infected for 2 h at low MOI, washed and then overlaid with 0.5% agarose (Invitrogen) medium. On day 11, cells were fixed by adding either 1% formaldehyde on top of the overlays or pure methanol directly to the cells. Cells were then, respectively, stained by applying a 0.5% crystal violet solution in 25% methanol or by performing 3,3′-diaminobenzidine (DAB) immunohistochemistry, probing for Ad fiber expression (4D2, Abcam). DAB reactions were enhanced by complementing the DAB solution (product D5905, Sigma-Aldrich) with $NiCl_2$ and $CuSO_4$ (both to a final concentration of 0.03% w/v).

Protein immunoblot analysis

Semiconfluent cultures of SKOV-3.pol-HA cells in 24-well plate wells ($\sim 1.5 \times 10^5$ cells/well) were incubated with 1000 VP/cell for 2 h. At 24 and 36 h after infection, cell lysates were made using 100 µl/well of RIPA lysis buffer (50 mM Tris-Cl, pH 7.5, 150 mM NaCl, 0.1% SDS, 0.5% deoxycholate and 1% NP40) supplemented with protease inhibitors. Lysate aliquots (10 µl) were boiled in reducing sample buffer and subjugated to sodium dodecyl sulfate–polyacrylamide gel electrophoreses (SDS–PAGE) using a two-layer resolving gel composed of 12% (top) and 15% (bottom) polyacrylamide. After electroblotting to polyvinylidene difluoride membranes, blots were probed by anti-fiber tail (4D2, Abcam) and anti-E1A [M73 (41)] monoclonals, a rabbit antiserum raised against an ADP peptide [P63-77 (42); a kind gift from Dr W. S. M. Wold] and matching horseradish peroxidase-coupled secondary antibodies. Immunologically detected proteins were visualized by enhanced chemiluminescence.

Reverse transcriptase–polymerase chain reaction

SKOV-3.PP cells in six-well plate wells ($\sim 5 \times 10^5$ cells/well) were infected at 1000 VP/cell for 1.5 h. At 8 and 24 h after infection, total RNA was isolated according to the Total RNA Isolation/NucleoSpin RNA II kit (Macherey-Nagel). First-strand cDNA synthesis, using oligo$(dT)_{20}$ primers, was performed on 250 ng of total RNA by the SuperScript III Reverse Transcriptase (Invitrogen) according to the manufacturer's instructions. One microliter portions of the reverse transcriptase reactions were subsequently used in PCRs using specific primer pairs listed in Supplementary Data.

Statistical analysis

The *P*-values assigned to the observed forward and reverse frequencies of a given minor variant indicate the probabilities of obtaining such frequencies or higher if they were to be due to sequencing errors. For the calculation of *P*-values, we assumed a Poisson distribution of errors, analogously to Wang *et al.* (43), and took as error rate estimates the 97.5th percentiles of the observed minor variant frequency distributions (see Supplementary Data for summary statistics). Usage of such high estimates of the error rate—instead of taking for instance the average of the minor variant frequency distributions—is thought to accommodate, at least partially, the presumed heterogeneity of the actual error rate (44).

RESULTS

Candidate mutator Ad polymerases and their ability to support Ad replication

To render Ad pol more error prone, we mutated residues putatively involved in maintaining polymerization fidelity. By extrapolation from data on other polymerase species, 19 Ad pol residues were selected for mutation (Figure 1). The selected residues roughly fall into two categories, those putatively involved with proofreading and those implicated in (geometric) selection of the incoming nucleotide. In total, 23 Ad pol mutants were generated (Supplementary Table S1), each engineered with a single amino acid substitution. Three of the targeted residues—N417, F421 and M689 (i.e. no. 4, 5 and 13 in Figure 1)—were represented by more than one mutant.

The newly engineered Ad pol mutants were assessed for their ability to support productive Ad replication. To this end, a *trans*-complementation assay was set up that involves lentiviral vector-mediated expression of Ad pol variants in cells, and the subsequent infection of these cells by a polymerase-defective reporter Ad vector (Supplementary Figure S1).

A first complementation assay revealed that nine of the Ad pol mutants supported productive replication of the polymerase-defective vector (Figure 2A shows green fluorescent protein (GFP) expression on day two for this experiment). The complementing mutants were T286I, N417A, F421Y, S506T, V585A, M689N, Y690F, D827A and S834E. Besides that they were associated with infected cells becoming brightly green fluorescent (indicating viral genome replication), these mutants also gave rise, eventually, to 'green comets' and/or plaques, demonstrating the production of viable progeny virus. Regarding the size and onset of such foci, marked variation was observed among the mutants, with M689N and Y690F lagging furthest behind. In summary of this assay and several subsequent, independent assays, all Ad pol mutants were assigned arbitrary complementation classes (Figure 2B).

Identification of mutator Ad polymerases

Ad pol mutants capable of supporting viral replication were subsequently analyzed for their proneness to cause mutations. For this purpose, a mutation-accumulation and sequencing scheme was devised for the direct assessment of mutational buildups in viruses replicated by virtue of the various Ad pol variants (Figure 3A). Central to this scheme is the employment of a MPS technology to perform 'deep sequencing' of virus DNA obtained from multi-clone virus pools.

To implement this strategy, we first established a safe maximum to the number of viral clones that could be pooled while permitting detection of single-clone mutations. For this, we performed a pilot sequencing run on a 3.1-kb DNA fragment spiked with several minority mutants (Table 1). Analysis of this run demonstrated

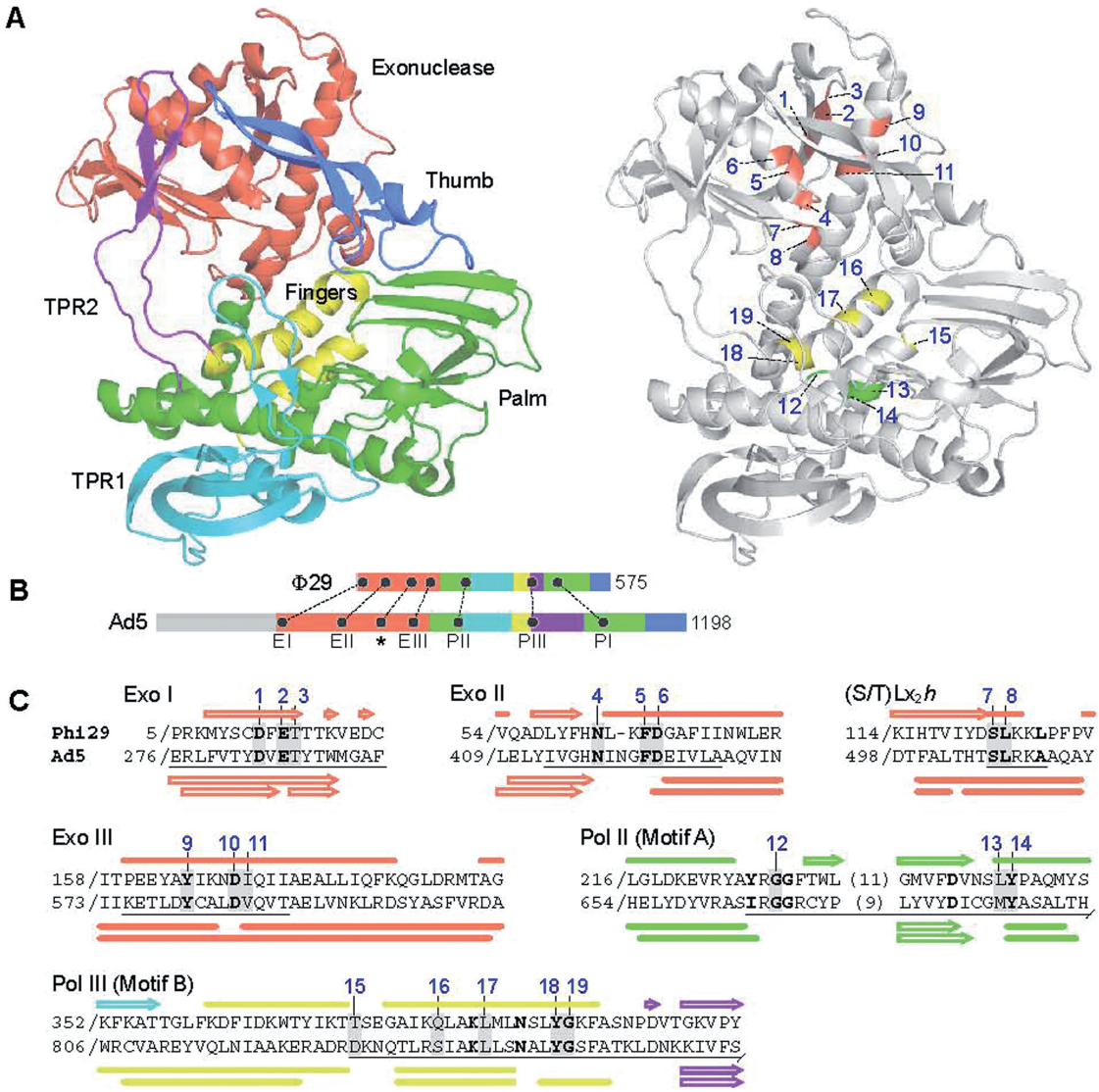

Figure 1. Ad pol residues targeted for mutation. Twenty-three single-amino acid substitution mutants of Ad pol were generated by mutation of nineteen selected residues implicated in governing replication fidelity (see also Supplementary Table S1). (**A**) The respective putative Φ29 homologues of the targeted Ad pol residues are depicted in the context of a Φ29 pol structure (Protein Data Bank code 1XI1) determined by Kamtekar *et al.* (47). The cartoon representation on the left shows the domain organization of Φ29 pol while the right diagram points out the targeted residues. Protein structure visualizations were by Polyview-3D (http://polyview.cchmc.org/) using image rendering by PyMol. (**B**) The mutated residues reside in several of the most highly conserved polymerase sequence motifs, the locations of which are shown in linear representations, to scale, of the Φ29 and Ad polymerases. Depicted are the 'Exo' motifs I, II and III (59), the (S/T)Lx$_2$*h* motif (46) (indicated by the asterisk) and the 'Pol' regions I, II and III (72), which are also, respectively, known as polymerase motifs C, A and B (73). (**C**) Sequence alignments of conserved motifs of Ad and Φ29 polymerases. The respective conserved motifs are underlined. Invariable residues are shown in bold face. Blue numbers point to the targeted Ad pol residues and their respective putative Φ29 homologues. Secondary structures known for Φ29 (47) and those predicted for Ad pol are, respectively, shown above and below the alignments. Closed bars indicate α-helices while open arrows represent β-strands. The upper and lower predictions for Ad pol were, respectively, by PredictProtein (http://www.predictprotein.org) and SABLE (http://sable.cchmc.org).

false positive-free mutation scoring using a minimal minor variant prevalence cutoff value of as low as 0.17% (Supplementary Figure S2), a cutoff that would theoretically allow a single-clone mutation to be detected in a pool of 588 even-sized clones. Based on this outcome, we opted to sequence a 6.5-kb fragment from virus pools containing ~50 clones each, thus allowing for some experimental variations in clone size and number.

All Ad pol mutants capable of Ad replication, including the parental HA-tagged Ad pol (i.e. pol-HA), were included in a mutation-accumulation experiment involving 10 serial passages of the polymerase-defective Ad vector (Figure 3A). However, passaging using the two most weakly complementing mutants, M689N and Y690F, was discontinued prematurely as these mutants proved unable to sustain multiple-round viral propagation. From the 10 times passaged virus populations and, additionally, from 2 non-passaged virus stocks, virus pools were prepared containing near 50 clones each. Subsequently, from each prepared viral pool, a 6.5-kb

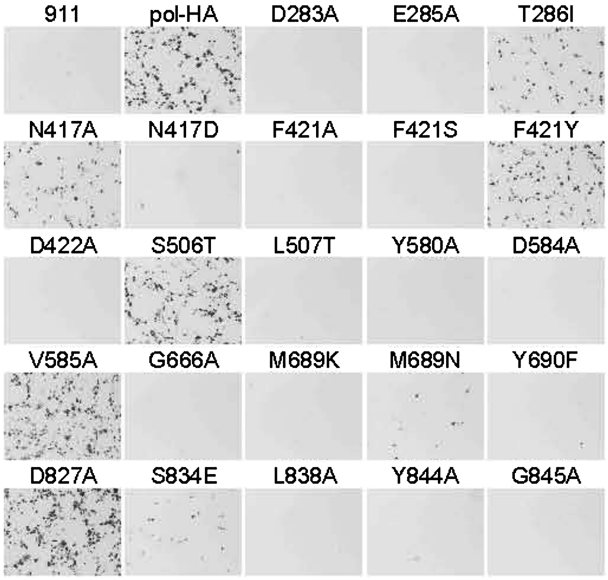

B

#	mutant	replicative ability	#	mutant	replicative ability
	pol-HA	+++	9	Y580A	-
1	D283A	-	10	D584A	-
2	E285A	-	11	V585A	+++
3	T286I	++	12	G666A	-
4	N417A	++	13	M689K	-
4	N417D	-	13	M689N	+
5	F421A	-	14	Y690F	+
5	F421S	-	15	D827A	+++
5	F421Y	++	16	S834E	+
6	D422A	-	17	L838A	-
7	S506T	+++	18	Y844A	-
8	L507T	-	19	G845A	-

Figure 2. Ability of candidate mutator Ad polymerases to support full-fledged Ad replication. (**A**) A *trans*-complementation system (see Supplementary Figure S1 for its components) was employed to assess the ability of the various Ad pol mutants to support Ad replication. Control 911 cells or 911 cell populations stably expressing the respective Ad pol variants were infected with a polymerase-defective Ad vector (AdGLΔPOL). The mutants' abilities to *trans*-complement AdGLΔPOL were assessed by monitoring vector-encoded reporter gene expression. The images show GFP fluorescence (inverted grayscale) at 2 days post-infection. 'pol-HA' stands for HA-tagged Ad pol, which is parental to the other Ad pol variants. The exposure time was the same for all pictures. Not discernible under this setting was the very weak GFP signal in infected cells that do not *trans*-complement the polymerase defect (e.g. 911 cells). (**B**) Summary of the abilities of the Ad pol mutants to complement the polymerase-defective vector. The numbers in the columns denoted by a pound symbol (#) correspond to the residue numbers assigned in Figure 1. The depicted complementation classes (–, +, ++ and +++) were arbitrarily assigned to reflect the differential patterns of complementation abilities observed for the mutants in several independent experiments (e.g. Figure 2A).

Ad genome fragment, spanning from the gene for pIX to that for pTP, was amplified and sequenced by MPS. After mapping of the short sequence reads, base substitutions were scored by imposing—on both the forwardly and reversely mapped read distributions—a local sequencing coverage depth requirement of 1200 and a minor variant frequency cutoff value of 0.25% (Supplementary Figure S3).

The base substitution scores found for the analyzed viral pools revealed that among the Ad pol mutants tested, all but one (i.e. S834E) displayed a degree of mutator activity (Figures 3B and C and Supplementary Table S2). Mutants T286I and F421Y were identified as the most distinctive mutators. With respect to the types of substitutions found, these two, but also the intermediate-level mutators S506T and D827A, exhibited a strong bias toward transitions, especially the transition involving the exchange of a G:C base pair for a A:T base pair (Figure 3D). Interestingly, the strongest of the identified mutators (T286I and F421Y) are both mutants of residues likely involved in stabilization of the displaced primer terminus at the exonuclease active site during proofreading (Supplementary Table S1). The putative homologues of these residues in Φ29 polymerase entertain direct contacts with single-stranded DNA (Figure 3E; 45–47).

Directed evolution using mutator polymerases yields virus pools with enhanced tumor cell killing potency

Next we investigated whether the identified mutator Ad polymerases could serve to facilitate the directed evolution of Ad. To this end, Ad pol variants N417A, F421Y, S506T, D827A, S834E and pol-HA, which together represent a wide range of mutator activities, were put into service in a directed evolution scheme involving multiple viral infection rounds on the human ovarian carcinoma cell line SKOV-3 (Figure 4A). Subjected to this selection scheme was an Ad5-based virus that, apart from the polymerase-disrupting deletion, is completely wild type. Further, the passaging conditions were chosen to strongly select for any faster growing mutants (see 'Materials and Methods' section for details).

Of the virus populations that had underwent the evolution procedure, several were found to have gained an enhanced cytolytic activity on the target SKOV-3 cells (Figure 4B). Interestingly, the observed cytotoxic potencies (Figure 4C) of the populations correlate with the mutator abilities (Figure 3C) of the Ad pol mutants used during bioselection. For example, directed evolution employing the highest level mutator, F421Y, proved to have yielded the most cytolytically potent virus population. Subsequent plaque size assessment on SKOV-3 cell monolayers further revealed the heterogeneity of the F421Y-bioselected population, with a considerable fraction of the viruses displaying a large plaque phenotype (Figure 4D).

Characterization of bioselected virus clones reveals overexpression of the adenovirus death protein

From the F421Y-bioselected pool, two individual viral clones (F421Y-c1 and F421Y-c2) were isolated and further characterized. In a cell killing assay, both clones displayed an increased ability to kill SKOV-3 cells (Figure 5A), with each registering a difference with the non-bioselected 'stock' virus of at least a 100-fold (Figure 5B). Furthermore, on SKOV-3 cell monolayers,

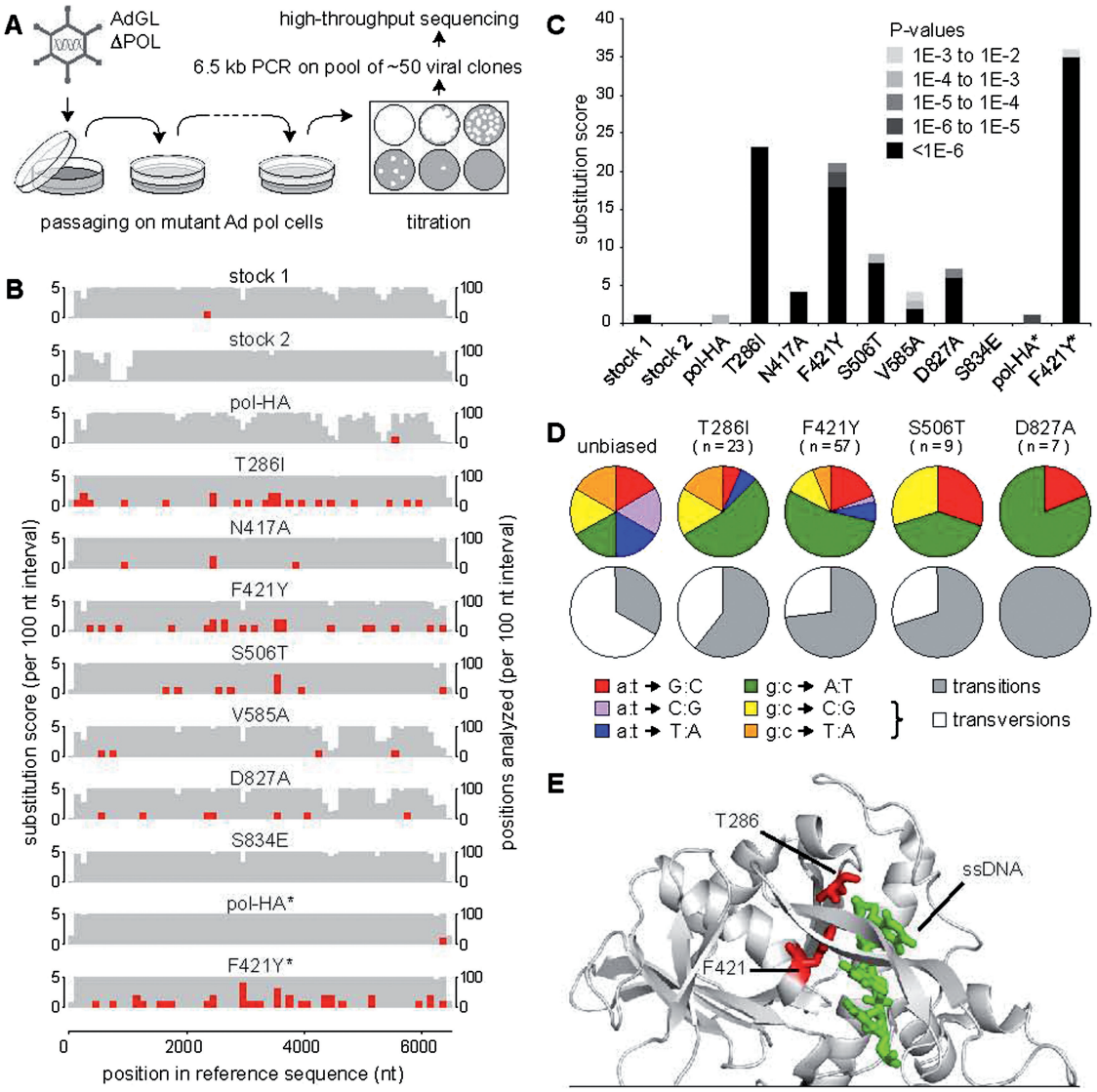

Figure 3. Identification of mutator Ad polymerases. (**A**) Mutation-accumulation and deep sequencing scheme. A polymerase-defective vector, AdGLΔPOL, was subjected to 10 serial infection rounds on candidate mutator Ad pol-expressing cell populations. For each passaged virus population, the potential mutation load buildup was assessed by deep sequencing (using a MPS technology) of a 6.5-kb virus DNA fragment obtained from a '50-clone' virus pool. After mapping of the sequence reads to the reference sequence, single-base substitutions were scored using a minor variant frequency cutoff value of 0.25% and a minimal sequencing depth requirement of 1200, both of which conditions were to be met for both the forwardly and reversely mapped read distributions. See Supplementary Figure S3 for details on mappings and minor variant detection. (**B**) Substitution score distributions over the length of the sequenced fragment. The grey background columns indicate, per 100-nt interval, the number of positions included in the analysis (i.e. the number of positions for which the minimal sequencing depth requirement was met). The red columns display the single-base substitutions scores. 'Stock 1' and 'stock 2' represent two independently prepared 50-clone pools of non-passaged viruses. Sample names marked with an asterisk (*) indicate the use of an alternative pooling method to obtain the '50-clone' pools. See text for details. (**C**) Total number of substitutions found per analyzed pool. For a given substitution, the assigned *P*-value range (shade of gray) relates to the higher of the two *P*-values estimated for the forward and reverse occurrence of that substitution. See the statistics section for *P*-value estimations. Further, see Supplementary Table S2 for the substitution scores expressed relative to the amount of DNA analyzed. (**D**) Base substitution spectra of the identified mutator Ad polymerases. The relative frequencies of the different types of substitutions were corrected for the GC content (of ~60%) of the analyzed sequence. (**E**) The Φ29 homologues of Ad Pol residues T286 and F421 have previously been shown to entertain direct contacts with single-stranded DNA (ssDNA) (47). The concerned residues are depicted, with side chains, in a cartoon representation of Φ29 pol, additionally displaying the cocrystallized ssDNA bound in the exonuclease active site. See Figure 1 for protein structure and visualization.

both clones were found to give rise, exclusively, to 'large' plaques (shown in Figure 5C for clone F421Y-c1). Apart from on SKOV-3, increased cell killing abilities were also observed on human breast (SKBR-3) and prostate (PC-3) carcinoma cell lines, and, to a lesser extent, on untransformed fibroblasts (VH10) (Supplementary Figure S4). In contrast, killing of a standard Ad producer cell line (911) was found to be either unaffected (F421Y-c1) or slightly attenuated (F421Y-c2).

Viral genome sequencing revealed seven and eight mutations for the respective clones, including one shared by the two (Figure 5D and Supplementary Table S3).

Table 1. Detection of spiked variants by deep sequencing[a]

Spike no.	Position	Base substitution	Spiked frequency (%)	Observed frequency (%)		*P*-values[b]	
				F	R	F	R
1	1393	A → C	25.0	16.9	14.8	<1E-14	<1E-14
	1395	A → C	25.0	22.0	14.0	<1E-14	<1E-14
2	1398	C → T	6.25	6.75	6.07	<1E-14	<1E-14
3	1790	A → G	1.56	1.78	1.84	<1E-14	<1E-14
	1792	C → T	1.56	1.71	3.22	<1E-14	<1E-14
4	1806	A → C	0.39	0.61	0.56	6.5E-13	<1E-14
5	2293	C → T	0.10	0.09	0.03	0.56	1.0
	2295	T → C	0.10	0.08	0.13	0.63	0.46

[a]The pilot deep sequencing run was performed on a spiked test sample consisting of a 3.1-kb DNA fragment spiked with several minority fragments, each containing a single or double nucleotide polymorphism. Depicted in this table are the frequencies with which the spiked variants occurred in the sequence read alignments. See Supplementary Data and Supplementary Figure S2 for more information on the sequencing run, the read alignment, and for an exemplification of minor variant detection.
[b]The *P*-values associated with the observed forward (F) and reverse (R) frequencies indicate the probabilities of obtaining such frequency levels or higher if they were due to sequencing errors. See the statistics section for the estimation of *P*-values.

All mutations were scrutinized for having any conceivable relevant functional consequences. Of those that were found to change primary protein structure (Supplementary Table S4), none were obvious candidates to underlie the observed phenotype. Further, with respect to non-protein-coding functions, only the single common mutation, at position 29 378 of the HAdV-5 genome, was identified by us as being potentially functionally relevant. The concerned mutation would affect a splice acceptor (SA) site preceding the exon encoding the adenovirus death protein (ADP) (31,42,48), a protein known to be required for efficient virus-mediated cell lysis and concomitant virus release (32).

Therefore, the ADP levels were investigated by immunoblot analysis at different time points after virus infection (Figure 5E). Importantly, both bioselected clones were found to exhibit highly elevated levels of ADP expression. Moreover, considerable levels of ADP were already detectable 24 h after infection, at which time the control virus showed no noticeable levels of ADP.

The overexpression of ADP correlates with altered splicing of E3 transcripts, not major late transcripts

The ADP gene, although embedded in the Ad E3 region, is considered an element of both the E3 and the major late (ML) transcription units (Figure 6, on the left). Early in infection, ADP is translated from two scarce E3 promoter-derived mRNAs, termed *d* and *e* (48,49). Later in infection, however, ADP is mostly translated from two highly abundant ML promoter-derived mRNAs, termed *d'* and *e'* (42). Importantly, splicing of both ADP mRNA types—E3 and ML-derived—critically involves utilization of the splice acceptor site found to be mutated in the bioselected viruses.

To provide evidence for any altered splicing dynamics involving ADP-encoding transcripts, we performed a reverse transcriptase–PCR analysis using primer sets allowing discrimination between the two ADP mRNA types (Figure 6). Control reactions were performed on cellular β-actin and viral E1A mRNAs (Supplementary Figure S5). Significantly, both bioselected clones exhibited markedly increased levels of the E3-derived ADP mRNAs (i.e. *d* and/or *e*), especially early and also late in infection. By marked contrast, no such elevations were observed for the ML-derived ADP mRNAs (*d'* and/or *e'*). Interestingly, the elevated levels of *d* and/or *e* mRNAs were found to be accompanied by an all-but-disappearance of the two normally abundant E3-derived mRNA species, *a* and *c* (48,49), which code for E3 proteins 6.7K and 19K. Furthermore, the normally lesser abundant mRNA *i*, encoding E3-12.5K, was also virtually absent. Thus, for both bioselected viruses, the splicing dynamics of E3 transcripts were found to be severely altered, displaying a marked shift in favor of the production of ADP-expressing mRNAs.

DISCUSSION

In the present study, we describe the development and validation of a conceptually new 'accelerated evolution' approach to Ad engineering that depends—for obtaining genetic diversity—on the error-prone viral genome replication achieved by engineered versions of the Ad polymerase. First, we report on the generation of several mutator Ad polymerases that sustain Ad replication. Next, we demonstrate that viral replication using such 'sloppy' Ad polymerases accelerates the adaptation to the selective pressures exerted by a directed evolution scheme aimed at increasing the oncolytic potency of Ad. Together, these findings demonstrate that mutator Ad polymerases can facilitate bioselection protocols for the isolation of Ads with new phenotypes. Interestingly, the specific application of our approach to enhance oncolytic Ad was found to yield viral mutants exhibiting high and early overexpression of the ADP, an outcome that is directly relevant for designing and engineering new, more potent oncolytic Ads (2,3,8–11). Importantly, neither the identified mutation nor any other mutations with similar implicated effects (i.e. early cell lysis due to untimely ADP overexpression) have previously been isolated in

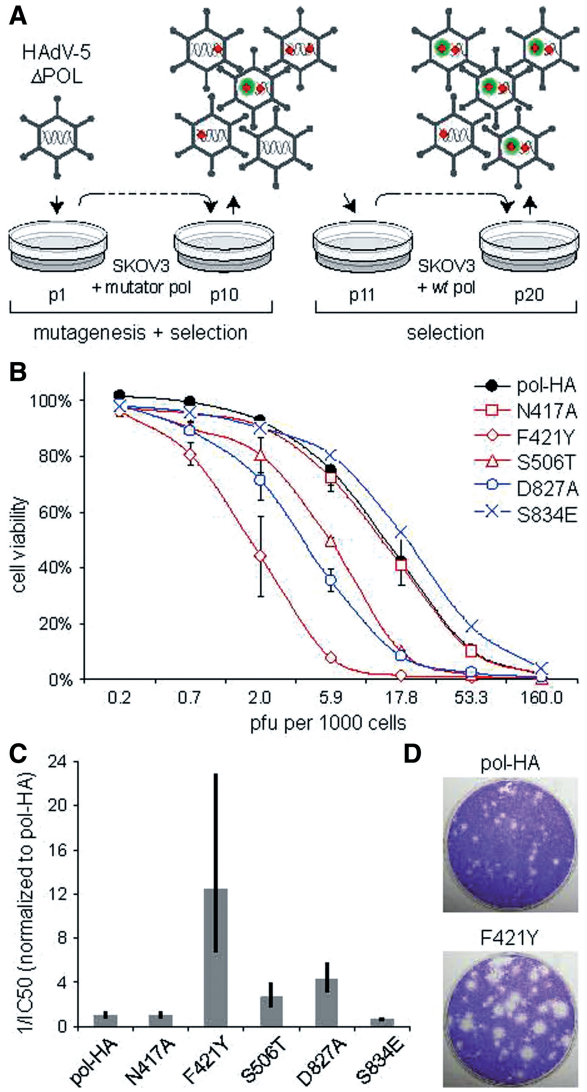

Figure 4. Directed evolution of Ad using mutator Ad polymerases. (**A**) Conceptual directed evolution scheme to achieve enhanced tumor cell killing. A HAdV-5-based virus, which otherwise from its polymerase disrupting deletion is fully wildtype in sequence, is subjected to iterative rounds of infection on tumor cell populations. Initial virus passaging on mutator Ad pol expressing cells results in genetically diverse pools from which viruses with an acquired growth advantage are enriched for in later passages. Red diamonds represent mutations. Green circles indicate an acquired selective advantage. (**B**) Virus populations bioselected using the indicated Ad pol variants were analyzed for cytotoxicity on their target cells. SKOV-3 cells were infected at the indicated MOI's and cell viabilities were assessed by WST-1 assay. Exonuclease domain mutants are shown in red, fingers domain mutants in blue. (**C**) A 12-fold decrease in IC_{50} was observed for the virus population bioselected using Ad pol mutator F421Y. The inversed IC_{50} values were calculated from the cytotoxicity assay above and normalized to that of the pol-HA-bioselected pool. Error bars indicate 95% confidence intervals. (**D**) A subpopulation of the F421Y-bioselected viruses forms large plaques on SKOV-3 cell monolayers. Cells were grown under an agarose layer and stained with crystal violet.

bioselection studies involving chemical or physical mutagens (12,14).

To render Ad pol more error prone, we mutated Ad pol residues implicated in maintaining polymerization accuracy. In general, replication fidelity of proofreading-proficient DNA polymerases is governed by two main mechanisms: incoming nucleotide selection—based mainly on nascent base pair geometry—and exonucleolytic excision of misinserted nucleotides, i.e. proofreading (50,51). Accordingly, we aimed to compromise either of these functions of Ad pol by introducing substitutions within conserved motifs of either the nucleotide-binding pocket or the exonuclease active site. Since for Ad pol there is only limited structure–function information, we drew heavily from data available on other polymerase species (Supplementary Table S1).

Most of the Ad pol mutants constructed in this study were unable to support full-fledged Ad replication. Very generally, mutants non-supportive of virus replication might be either directly or indirectly—i.e. through global structural changes—impaired with respect to one or more essential aspects of viral genome replication (e.g. DNA binding, protein-primed initiation, transition between initiation and elongation, polymerase catalytic activity, strand-displacement and processivity). Strikingly, among the defective mutants were all those with substitutions of the universally conserved exonuclease residues contributing to the metal ion binding framework of the exonuclease active site (i.e. mutants D283A, E285A, D422A, Y580A and D584A). Previously, analogous substitutions in other viral polymerases—those of RB69, HSV and CMV—did prove compatible with virus replication (52–54). In contrast, for Φ29 polymerase, the concerned residues are known not only to be vital for exonucleolytic activity but also to play an essential role in strand-displacement functionality during polymerization (55,56). Speculatively, our data on Ad pol reflects a similar such dual role for these invariantly conserved residues.

To reveal any mutator activities of Ad pol mutants that were supportive of Ad replication, we performed 'deep sequencing'—by MPS—on pools of viruses replicated by the respective polymerases. Previously, deep sequencing has proven a powerful means to detect low-prevalence mutations in heterogeneous samples, such as virus populations, tumors and/or pooled samples (43,44,57,58). Here, we exploited Illumina's MPS technology to detect point mutations in a 6.5-kb viral DNA fragment obtained from near 50-clone pools of viruses that had undergone 10 viral replication rounds. Importantly, this approach enabled us to obtain direct molecular evidence for any mutational buildups in a procedural context that, with its multiple-round viral passaging on cells, resembles a directed evolution regime.

Of the Ad pol mutants that sustained multiple-round viral replication, several displayed a degree of mutator activity. The strongest of these were T286I and F421Y, respectively, mutants of exonuclease motifs I and II (59). These two mutators, as well as the weaker mutator N417A, carry replacements of residues whose counterparts in Φ29 are important for primer terminus stabilization—putatively through direct binding (47)—at the exonuclease active site during proofreading (45,46). Another of the identified mutators, S506T, carries a substitution within the 'S/TLx$_2$*h*' motif of the exonuclease domain (46). Akin to the above mutants, its mutator

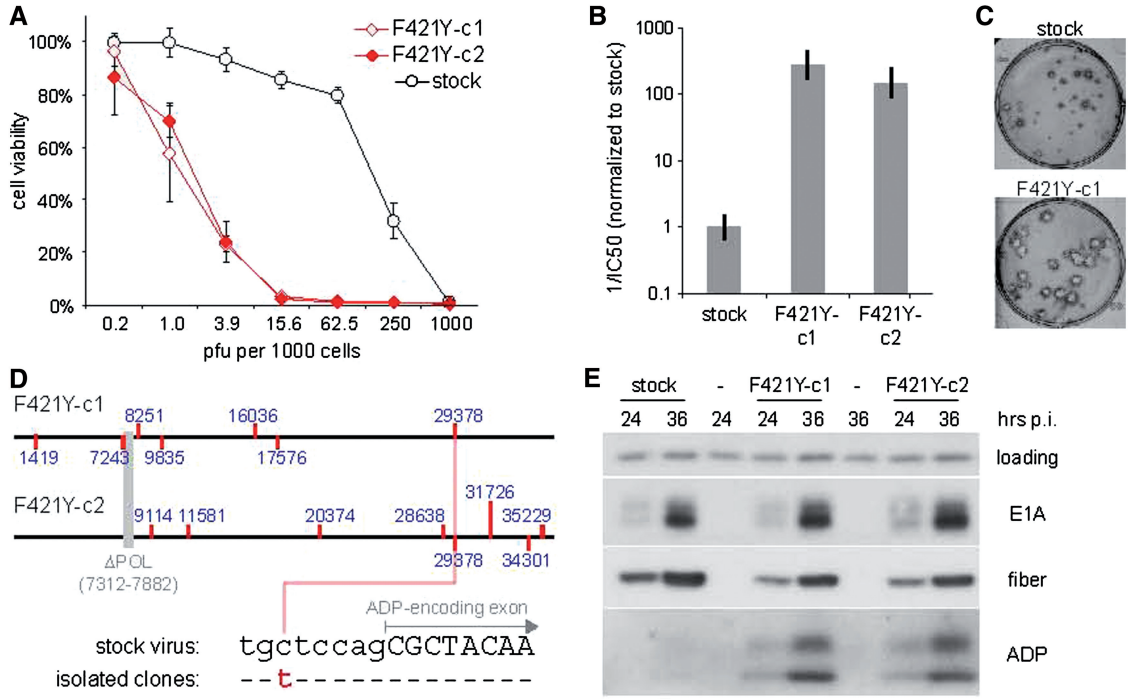

Figure 5. Characterization of isolated bioselected viral clones F421Y-c1 and F421Y-c2. Two clones with a large plaque phenotype were isolated from the F421Y-bioselected virus population and further characterized. Cell killing ability on SKOV-3 cells was assessed by a cytotoxicity (**A** and **B**) and a plaque size (**C**) assay. Error bars for the inversed IC_{50} columns indicate 95% confidence intervals. For the plaque size assay, cells were grown under an agarose layer and were visualized by immunohistochemistry for Ad fiber protein expression. See Supplementary Figure S4 for cell killing abilities on other (tumor) cell lines. (**D**) Sequencing of the genomes of the two clones revealed a shared mutation located within the splice acceptor site of the ADP-encoding exon. Mutations are indicated by red ticks. Blue numbers correspond to the respective positions in the wildtype HAdV-5 genome (accession no. AC_000008). See Supplementary Tables S3 and S4 for all detected mutations and their predicted consequences for primary protein structures. (**E**) The bioselected clones show highly increased levels of ADP expression. SKOV-3 cells were harvested for protein immunoblot analysis at 24 and 36 h after their infection. Blots were immunologically probed for Ad proteins E1A, fiber and ADP.

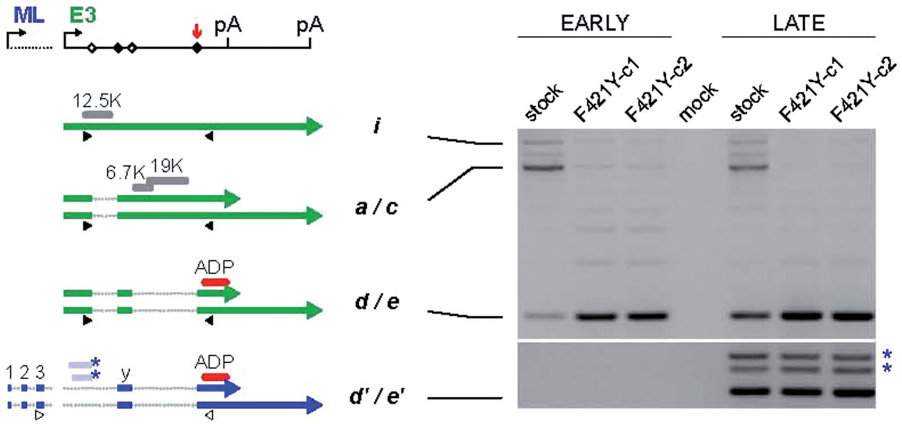

Figure 6. Viral clones F421Y-c1 and F421Y-c2 show a deregulated E3 splicing pattern strongly favoring the production of ADP-encoding mRNAs. RT–PCRs were performed with primer sets discriminating between E3 and ML promoter-derived ADP-encoding mRNAs. These primer sets, respectively, indicated by closed and open triangles, have a common reverse primer (targeting the ADP coding sequence) but consist of different forward primers (targeting the first E3 exon and the 3rd leader of the ML tripartite leader sequence). Depicted are all mRNA species recognized by these primer sets [according to Ad2 and Ad5 transcritption maps (42,48,49)]. E3 mRNAs (i.e. *a*, *c*, *d*, *e* and *i*) are shown in green while ML mRNAs (i.e. *d'* and *e'*) are depicted in blue. Within the E3 transcription unit, the splice donor and acceptor sites involved with splicing of the shown mRNAs are, respectively, depicted by open and closed diamonds. The red arrow points to the splice site found to be mutated in the bioselected clones. Further depicted are the relevant polyadenylation signals (pA), E3 proteins (12.5K, 6.7K, 19K and ADP) and leader sequences of the ML transcription unit (1, 2, 3 and y). The RT–PCR results show highly increased levels of E3- but not ML-derived ADP mRNAs. Furthermore, the altered alternative splicing of E3 transcripts was found to go at the expense of mRNA species *a*/*c* and *i*. The two asterisks next to the gel-image denote newly identified minority ML-derived ADP mRNAs. These variants presumably carry instead of the y-leader sequence one of two longer 'x-leader' exons (also denoted by asterisks) that would overlap with the first E3 exon. For control RT–PCRs on cellular β-actin and viral E1A mRNAs see Supplementary Figure S5.

activity could result from a lesser ability to stabilize primer termini during proofreading. However, considering the buried state of the homologous residue in Φ29 polymerase (47), any such impact might be through indirect effects. Further, also D827A was identified as an intermediate-strength mutator. Residue D827, which is non-highly conserved, is putatively located on a loop structure connecting two α-helices of the fingers domain (see Figure 1, residue no. 15). Thus, the D827A substitution might have indirect effects on incoming nucleotide selection, perhaps through an altered or more flexible relative positioning of the two helices, as has been suggested for mutator activity-yielding substitutions at similar positions in *Pyrococcus furiosus* polymerase (60).

The mutation rates—at the viral level—achieved by Ad pol mutants T286I and F421Y are within the range of those reported for highly evolvable RNA viruses, indicating perhaps a particular suitability of these mutants for directed Ad evolution. For the two pools of F421Y mutant-replicated viruses (i.e. pools 'F421Y' and 'F421Y*'), the observed respective substitution loads were 73 and 100 per million base pairs (Supplementary Table S2). These numbers would correspond to a substitution rate, per viral passage, of 0.26 and 0.36 per Ad5 genome length equivalent (i.e. 36 kb). Considering that the latter of these measures is probably the more accurate (given the pooling methods used) and, furthermore, that these measures only represent the non-lethal mutations, we expect that viruses replicated by the F421Y mutant—and, by analogy, the T286I mutant—underwent genomic mutation rates of at least, but probably greater than, 0.4 per viral generation. By comparison, for several 'rapidly evolving' riboviruses (i.e. measles virus, poliovirus, rhinovirus and vesicular stomatitis virus), estimates for the per-genome per-generation mutation rate ranged from 0.26 to 2.3 (61). Likewise, the genomic mutation rates for the fast adapting retroviruses have been estimated at a mean of 0.3 per viral generation (62).

Mutator Ad polymerases successfully served in a directed evolution regime aimed at increasing the oncolytic potency of Ad. Ad pol mutants were employed to replicate Ad—through *trans*-complementation—in a viral passaging scheme performed on the human ovarian carcinoma cell line SKOV-3. Resultant 'bioselected' virus populations that had undergone replication by either intermediate level (S506T and D827A) or strong (F421Y) mutators were found to have gained an increased cytolytic activity on the target cell line. In contrast, populations subjected to replication by weak and non-mutators (i.e. N417A and S834E, respectively) showed no evidence of any fitness gain relative to the control passaged virus population. These outcomes, combined with the mutation loads found in individual bioselected clones, demonstrate that engineered mutator Ad polymerases can be used to generate the genetic diversity needed to effectively facilitate directed Ad evolution.

A common mutation seen in the two isolated bioselected clones (at position 29 378 of the HAdV-5 genome) affects a splice acceptor site known to be critically involved in the generation of ADP-encoding mRNAs (42,48). Given that ADP is crucial for efficient cell death and virus release (32), its implication with the observed enhanced cytotoxic phenotype is highly conceivable. The ADP gene resides in the E3 region and is accordingly expressed, albeit relatively scarcely, from E3 promoter-derived mRNAs early in infection (42,48,49). However, ADP is additionally and much more abundantly expressed from major late promoter-derived transcripts arising later in infection (>24 h p.i.) (42). Both isolated virus clones exhibited dramatically elevated levels of ADP, the overproduction of which already became noticeable early in infection. Furthermore, the splicing pattern of E3 transcripts was found to be severely affected, with the generation of ADP-encoding mRNAs being strongly favored at the expense of other E3 mRNA species. In contrast, the levels of ADP-encoding mRNAs originating from the major late promoter were relatively unaffected. Thus, these data indicate an untimely expression of ADP that is mechanistically attributable to an increased utilization—within E3 transcripts—of the mutated splice acceptor site preceding the ADP-encoding sequence.

Several previous studies that aimed to enhance Ad's oncolytic potency have rationally sought to overexpress ADP or other cell death-inducing proteins (2,3,6–11). The ADP-overexpressing viruses generated in these studies were found to exhibit accelerated cell-to-cell viral spread *in vitro*, and improved antitumor efficacy *in vivo*. These data thus illustrate the direct relevance of our bioselected, ADP-overexpressing viral mutants for oncolytic virotherapy. Notably, the 'ADP splice-site mutation' identified here may be directly implementable in the context of existing designs of oncolytic Ad vectors. For example, vectors already endowed with tumor specificity might greatly benefit from the anticipated boost in oncolytic potency conferred by this mutation.

Taken together, our data validate a new, evolution-based bioengineering approach for Ad. In general, evolution-based engineering methods—i.e. methods based on genetic diversification and phenotypic selection—are powerful tools to isolate viruses with new or improved properties (63). Important advantages of these 'random' engineering methods over rational design are that they do not require an in-depth mechanistic insight and, furthermore, that they have the potential to yield unanticipated solutions to virus engineering problems. Existing viral random engineering methods can be divided into two general types: conventional forward genetics, which employs mutagens to bring about genome-wide mutagenesis, and the more modern approaches that combine *in vitro* genetic diversification techniques (64,65) with viral library-based selection (63). Both of these methods have been applied with some success to Ads in the past (12-14,66,67). However, the usefulness of the latter of these methods for Ad engineering has—in comparison to that for AAV (68) or retrovirus (69) engineering—been limited due to the difficulty of generating sufficiently complex adenoviral libraries. Recently, there has been significant progress in this respect. Different studies explored a site-specific recombination system to transfer plasmid-based Ad fiber-peptide libraries directly into replicating Ads, thus bypassing major efficiency bottlenecks in Ad library generation (i.e.

large genome handling and transfection, and virus rescue from naked viral DNA) (66,67).

With the ability to achieve genome-wide genetic diversification, our viral polymerase-based approach bears some similarity to traditional strategies relying on mutagens. However, major conceptual and practical distinctions exist. First, while mutator viral polymerases cause mutations directly, mutagens do so through the infliction of DNA damage. This is of relevance because not all mutagen-induced DNA lesions—like cross-links produced by nitrous acid (70) —can be bypassed by polymerases or repaired (16,70). In this regard, the greater part of the lethality seen after mutagen exposure may be due to collateral viral inactivation—consequential to irresolvable DNA lesions and damaged protein components—rather than bona fide genetic mutations (17). Importantly, this mutagen-associated excess lethality compromises the effective complexities of the diversified populations (17). While these issues are not so much a problem in single mutational-pulse experiments (because the amount of input virus can be chosen sufficiently high), they thwart schemes involving repeated mutagenic treatments, e.g. following each replication round. This points to a second, very important distinctive aspect of the polymerase-based approach, namely that it naturally allows repeated rounds of mutagenesis and selection. Thus, our approach is particularly suitable for directed evolution procedures involving multiple mutagenic viral passages, allowing for the possibility of generating compound mutants.

The Ad engineering approach described here is essentially an accelerated form of evolution that, regarding viral mutation rate levels, matches RNA virus evolution (see above). This is of interest because it is well established that the rapid evolution of RNA viruses can be effectively exploited for directed evolution purposes. For example, many of the most promising oncolytic riboviruses were the (coincidental) result of multiple-passage adaptation to growth in tissue culture cells (19). Furthermore, there are many recent examples where the adaptabilities of riboviruses (such as rhinovirus, coxsackievirus, vesicular stomatitis virus, sindbis virus, tick-borne encephalitis virus and avian influenza) and retroviruses (HIV-I and MLV) have been deliberately exploited to achieve specific vectorological goals. For example, riboviruses were evolved to exhibit enhanced target cell killing (18), altered or expanded receptor specificity (18,20,27,28), altered protease specificity (21) and ability to grow in cells of other host species (22,23). Likewise, retrovirus adaptability has been exploited to optimize viral envelope glycoprotein-pseudotyped recombinant vectors (24–26). Thus, with appropriate selective conditions imposed, similar aims for Ad may be achievable by our rapid evolution approach. In this regard, a general aim would be to restore or optimize recombinant Ad vectors (e.g. retargeted vectors) with impaired or limited function. Further, a captivating specific goal would be to generate human Ad derivatives capable of productive infection of mouse cells. Such mouse-adapted viruses would help realization of a permissive mouse model for replication-competent human Ad infection, potentially an invaluable tool for preclinical safety and efficacy studies (71).

The mutator polymerase-based Ad engineering approach presented here should be easily implementable by others, offering great practical flexibility and choice regarding the design of evolution regimes. There are two general ways recommended to adopt the system. Mutator viral polymerases might be stably expressed in target cells—e.g. using lentiviral vectors, as in our study—or, alternatively, be encoded for by the virus itself. In the first approach, one might consider using instead of a polymerase-defective virus, a polymerase-proficient one. This would save the reintroduction of the polymerase gene into any promising viral mutants (or, conversely, the introduction of promising acquired mutations into a *wt* virus). However, in such a setting, due to the co-presence of *wt* and mutator polymerases within the infected cells, the level of mutation is likely to be compromised somewhat. Therefore, it may be advantageous for this purpose to use Ad pol mutants exhibiting hyper-mutator phenotypes. In this regard, our unpublished data shows that some of the viable polymerase mutations identified in this study can be combined, thereby generating yet higher level mutators. Finally, the second approach to adopt the system—introduction of the mutator polymerase gene into the virus genome—might be especially attractive in the context of *in vivo* directed evolution schemes.

SUPPLEMENTARY DATA

Supplementary Data are available at NAR Online.

ACKNOWLEDGEMENTS

We thank William Wold and Ann Tollefson (St Louis University, St Louis, MO, USA) for providing the ADP antibody. Jeroen Bakker (Amsterdam Medical Center, Amsterdam, The Netherlands) is acknowledged for providing technical assistance. Peter C. van der Vliet (University Medical Center Utrecht, Utrecht, The Netherlands) is thanked for critical reading of the manuscript and for giving valuable suggestions.

FUNDING

European Union through the 6th Framework Program GIANT (contract no. 512087). Funding for open access charge: Leiden University Medical Center and European Union through the 6th Framework Program GIANT (contract no. 512087).

Conflict of interest statement. None declared.

REFERENCES

1. Parato,K.A., Senger,D., Forsyth,P.A. and Bell,J.C. (2005) Recent progress in the battle between oncolytic viruses and tumours. *Nat. Rev. Cancer*, **5**, 965–976.
2. Alemany,R. (2009) Designing adenoviral vectors for tumor-specific targeting. *Methods Mol. Biol.*, **542**, 57–74.

3. Toth,K., Dhar,D. and Wold,W.S. (2010) Oncolytic (replication-competent) adenoviruses as anticancer agents. *Expert. Opin. Biol. Ther.*, **10**, 353–368.
4. DeWeese,T.L., van der,P.H., Li,S., Mikhak,B., Drew,R., Goemann,M., Hamper,U., DeJong,R., Detorie,N., Rodriguez,R. *et al.* (2001) A phase I trial of CV706, a replication-competent, PSA selective oncolytic adenovirus, for the treatment of locally recurrent prostate cancer following radiation therapy. *Cancer Res.*, **61**, 7464–7472.
5. Khuri,F.R., Nemunaitis,J., Ganly,I., Arseneau,J., Tannock,I.F., Romel,L., Gore,M., Ironside,J., MacDougall,R.H., Heise,C. *et al.* (2000) a controlled trial of intratumoral ONYX-015, a selectively-replicating adenovirus, in combination with cisplatin and 5-fluorouracil in patients with recurrent head and neck cancer. *Nat. Med.*, **6**, 879–885.
6. Sauthoff,H., Pipiya,T., Heitner,S., Chen,S., Norman,R.G., Rom,W.N. and Hay,J.G. (2002) Late expression of p53 from a replicating adenovirus improves tumor cell killing and is more tumor cell specific than expression of the adenoviral death protein. *Hum. Gene Ther.*, **13**, 1859–1871.
7. van Beusechem,V.W., van den Doel,P.B., Grill,J., Pinedo,H.M. and Gerritsen,W.R. (2002) Conditionally replicative adenovirus expressing p53 exhibits enhanced oncolytic potency. *Cancer Res.*, **62**, 6165–6171.
8. Barton,K.N., Paielli,D., Zhang,Y., Koul,S., Brown,S.L., Lu,M., Seely,J., Kim,J.H. and Freytag,S.O. (2006) Second-generation replication-competent oncolytic adenovirus armed with improved suicide genes and ADP gene demonstrates greater efficacy without increased toxicity. *Mol. Ther.*, **13**, 347–356.
9. Yun,C.O., Kim,E., Koo,T., Kim,H., Lee,Y.S. and Kim,J.H. (2005) ADP-overexpressing adenovirus elicits enhanced cytopathic effect by induction of apoptosis. *Cancer Gene Ther.*, **12**, 61–71.
10. Doronin,K., Toth,K., Kuppuswamy,M., Ward,P., Tollefson,A.E. and Wold,W.S. (2000) Tumor-specific, replication-competent adenovirus vectors overexpressing the adenovirus death protein. *J. Virol.*, **74**, 6147–6155.
11. Ramachandra,M., Rahman,A., Zou,A., Vaillancourt,M., Howe,J.A., Antelman,D., Sugarman,B., Demers,G.W., Engler,H., Johnson,D. *et al.* (2001) Re-engineering adenovirus regulatory pathways to enhance oncolytic specificity and efficacy. *Nat. Biotechnol.*, **19**, 1035–1041.
12. Yan,W., Kitzes,G., Dormishian,F., Hawkins,L., Sampson-Johannes,A., Watanabe,J., Holt,J., Lee,V., Dubensky,T., Fattaey,A. *et al.* (2003) Developing novel oncolytic adenoviruses through bioselection. *J. Virol.*, **77**, 2640–2650.
13. Subramanian,T., Vijayalingam,S. and Chinnadurai,G. (2006) Genetic identification of adenovirus type 5 genes that influence viral spread. *J. Virol.*, **80**, 2000–2012.
14. Gros,A., Martinez-Quintanilla,J., Puig,C., Guedan,S., Mollevi,D.G., Alemany,R. and Cascallo,M. (2008) Bioselection of a gain of function mutation that enhances adenovirus 5 release and improves its antitumoral potency. *Cancer Res.*, **68**, 8928–8937.
15. Kuhn,I., Harden,P., Bauzon,M., Chartier,C., Nye,J., Thorne,S., Reid,T., Ni,S., Lieber,A., Fisher,K. *et al.* (2008) Directed evolution generates a novel oncolytic virus for the treatment of colon cancer. *PLoS One*, **3**, e2409.
16. Freese,E.B. and Freese,E. (1964) Two separable effects of hydroxylamine on transforming DNA. *Proc. Natl Acad. Sci. USA*, **52**, 1289–1297.
17. Bull,J.J. (2008) The optimal burst of mutation to create a phenotype. *J. Theor. Biol.*, **254**, 667–673.
18. Gao,Y., Whitaker-Dowling,P., Watkins,S.C., Griffin,J.A. and Bergman,I. (2006) Rapid adaptation of a recombinant vesicular stomatitis virus to a targeted cell line. *J. Virol.*, **80**, 8603–8612.
19. Russell,S.J. (2002) RNA viruses as virotherapy agents. *Cancer Gene Ther.*, **9**, 961–966.
20. Klimstra,W.B., Ryman,K.D. and Johnston,R.E. (1998) Adaptation of Sindbis virus to BHK cells selects for use of heparan sulfate as an attachment receptor. *J. Virol.*, **72**, 7357–7366.
21. Fischl,W., Elshuber,S., Schrauf,S. and Mandl,C.W. (2008) Changing the protease specificity for activation of a flavivirus, tick-borne encephalitis virus. *J. Virol.*, **82**, 8272–8282.
22. Harris,J.R. and Racaniello,V.R. (2003) Changes in rhinovirus protein 2C allow efficient replication in mouse cells. *J. Virol.*, **77**, 4773–4780.
23. Gabriel,G., Dauber,B., Wolff,T., Planz,O., Klenk,H.D. and Stech,J. (2005) The viral polymerase mediates adaptation of an avian influenza virus to a mammalian host. *Proc. Natl Acad. Sci. USA*, **102**, 18590–18595.
24. Bontjer,I., Land,A., Eggink,D., Verkade,E., Tuin,K., Baldwin,C., Pollakis,G., Paxton,W.A., Braakman,I., Berkhout,B. *et al.* (2009) Optimization of human immunodeficiency virus type 1 envelope glycoproteins with V1/V2 deleted, using virus evolution. *J. Virol.*, **83**, 368–383.
25. Logg,C.R., Baranick,B.T., Lemp,N.A. and Kasahara,N. (2007) Adaptive evolution of a tagged chimeric gammaretrovirus: identification of novel cis-acting elements that modulate splicing. *J. Mol. Biol.*, **369**, 1214–1229.
26. Barsov,E.V., Payne,W.S. and Hughes,S.H. (2001) Adaptation of chimeric retroviruses in vitro and in vivo: isolation of avian retroviral vectors with extended host range. *J. Virol.*, **75**, 4973–4983.
27. Reischl,A., Reithmayer,M., Winsauer,G., Moser,R., Gosler,I. and Blaas,D. (2001) Viral evolution toward change in receptor usage: adaptation of a major group human rhinovirus to grow in ICAM-1-negative cells. *J. Virol.*, **75**, 9312–9319.
28. Johansson,E.S., Xing,L., Cheng,R.H. and Shafren,D.R. (2004) Enhanced cellular receptor usage by a bioselected variant of coxsackievirus a21. *J. Virol.*, **78**, 12603–12612.
29. Liu,H., Naismith,J.H. and Hay,R.T. (2003) Adenovirus DNA replication. *Curr. Top Microbiol. Immunol.*, **272**, 131–164.
30. King,A.J., Teertstra,W.R., Blanco,L., Salas,M. and van der Vliet,P.C. (1997) Processive proofreading by the adenovirus DNA polymerase. Association with the priming protein reduces exonucleolytic degradation. *Nucleic Acids Res.*, **25**, 1745–1752.
31. Wold,W.S., Cladaras,C., Magie,S.C. and Yacoub,N. (1984) Mapping a new gene that encodes an 11,600-molecular-weight protein in the E3 transcription unit of adenovirus 2. *J. Virol.*, **52**, 307–313.
32. Tollefson,A.E., Scaria,A., Hermiston,T.W., Ryerse,J.S., Wold,L.J. and Wold,W.S. (1996) The adenovirus death protein (E3-11.6K) is required at very late stages of infection for efficient cell lysis and release of adenovirus from infected cells. *J. Virol.*, **70**, 2296–2306.
33. Fallaux,F.J., Kranenburg,O., Cramer,S.J., Houweling,A., van Ormondt,H., Hoeben,R.C. and van der Eb,A.J. (1996) Characterization of 911: a new helper cell line for the titration and propagation of early region 1-deleted adenoviral vectors. *Hum. Gene Ther.*, **7**, 215–222.
34. Klein,B., Pastink,A., Odijk,H., Westerveld,A. and van der Eb,A.J. (1990) Transformation and immortalization of diploid xeroderma pigmentosum fibroblasts. *Exp. Cell Res.*, **191**, 256–262.
35. Barry,S.C., Harder,B., Brzezinski,M., Flint,L.Y., Seppen,J. and Osborne,W.R. (2001) Lentivirus vectors encoding both central polypurine tract and posttranscriptional regulatory element provide enhanced transduction and transgene expression. *Hum. Gene Ther.*, **12**, 1103–1108.
36. Uil,T.G., de Vrij,J., Vellinga,J., Rabelink,M.J., Cramer,S.J., Chan,O.Y., Pugnali,M., Magnusson,M., Lindholm,L., Boulanger,P. *et al.* (2009) A lentiviral vector-based adenovirus fiber-pseudotyping approach for expedited functional assessment of candidate retargeted fibers. *J. Gene Med.*, **11**, 990–1004.
37. Murakami,P. and McCaman,M.T. (1999) Quantitation of adenovirus DNA and virus particles with the PicoGreen fluorescent Dye. *Anal. Biochem.*, **274**, 283–288.
38. Ossowski,S., Schneeberger,K., Clark,R.M., Lanz,C., Warthmann,N. and Weigel,D. (2008) Sequencing of natural strains of Arabidopsis thaliana with short reads. *Genome Res.*, **18**, 2024–2033.
39. Schneeberger,K., Hagmann,J., Ossowski,S., Warthmann,N., Gesing,S., Kohlbacher,O. and Weigel,D. (2009) Simultaneous alignment of short reads against multiple genomes. *Genome Biol.*, **10**, R98.
40. Zerbino,D.R. and Birney,E. (2008) Velvet: algorithms for de novo short read assembly using de Bruijn graphs. *Genome Res.*, **18**, 821–829.

41. Harlow,E., Franza,B.R. Jr and Schley,C. (1985) Monoclonal antibodies specific for adenovirus early region 1A proteins: extensive heterogeneity in early region 1A products. *J.Virol.*, **55**, 533–546.
42. Tollefson,A.E., Scaria,A., Saha,S.K. and Wold,W.S. (1992) The 11,600-MW protein encoded by region E3 of adenovirus is expressed early but is greatly amplified at late stages of infection. *J. Virol.*, **66**, 3633–3642.
43. Wang,C., Mitsuya,Y., Gharizadeh,B., Ronaghi,M. and Shafer,R.W. (2007) Characterization of mutation spectra with ultra-deep pyrosequencing: application to HIV-1 drug resistance. *Genome Res.*, **17**, 1195–1201.
44. Out,A.A., van Minderhout,I.J., Goeman,J.J., Ariyurek,Y., Ossowski,S., Schneeberger,K., Weigel,D., van Galen,M., Taschner,P.E., Tops,C.M. *et al.* (2009) Deep sequencing to reveal new variants in pooled DNA samples. *Hum. Mutat.*, **30**, 1703–1712.
45. de Vega,M., Lazaro,J.M., Salas,M. and Blanco,L. (1996) Primer-terminus stabilization at the 3′-5′ exonuclease active site of phi29 DNA polymerase. Involvement of two amino acid residues highly conserved in proofreading DNA polymerases. *EMBO J.*, **15**, 1182–1192.
46. de Vega,M., Lazaro,J.M., Salas,M. and Blanco,L. (1998) Mutational analysis of phi29 DNA polymerase residues acting as ssDNA ligands for 3′-5′ exonucleolysis. *J. Mol. Biol.*, **279**, 807–822.
47. Kamtekar,S., Berman,A.J., Wang,J., Lazaro,J.M., de Vega,M., Blanco,L., Salas,M. and Steitz,T.A. (2004) Insights into strand displacement and processivity from the crystal structure of the protein-primed DNA polymerase of bacteriophage phi29. *Mol. Cell*, **16**, 609–618.
48. Cladaras,C., Bhat,B. and Wold,W.S. (1985) Mapping the 5′ ends, 3′ ends, and splice sites of mRNAs from the early E3 transcription unit of adenovirus 5. *Virology*, **140**, 44–54.
49. Chow,L.T., Broker,T.R. and Lewis,J.B. (1979) Complex splicing patterns of RNAs from the early regions of adenovirus-2. *J. Mol. Biol.*, **134**, 265–303.
50. Kunkel,T.A. (2004) DNA replication fidelity. *J. Biol. Chem.*, **279**, 16895–16898.
51. Patel,P.H. and Loeb,L.A. (2001) Getting a grip on how DNA polymerases function. *Nat. Struct. Biol.*, **8**, 656–659.
52. Bebenek,A., Dressman,H.K., Carver,G.T., Ng,S., Petrov,V., Yang,G., Konigsberg,W.H., Karam,J.D. and Drake,J.W. (2001) Interacting fidelity defects in the replicative DNA polymerase of bacteriophage RB69. *J. Biol. Chem.*, **276**, 10387–10397.
53. Hwang,Y.T., Liu,B.Y., Coen,D.M. and Hwang,C.B. (1997) Effects of mutations in the Exo III motif of the herpes simplex virus DNA polymerase gene on enzyme activities, viral replication, and replication fidelity. *J. Virol.*, **71**, 7791–7798.
54. Chou,S. and Marousek,G.I. (2008) Accelerated evolution of maribavir resistance in a cytomegalovirus exonuclease domain II mutant. *J. Virol.*, **82**, 246–253.
55. Esteban,J.A., Soengas,M.S., Salas,M. and Blanco,L. (1994) 3′–>5′ exonuclease active site of phi 29 DNA polymerase. Evidence favoring a metal ion-assisted reaction mechanism. *J. Biol. Chem.*, **269**, 31946–31954.
56. Soengas,M.S., Esteban,J.A., Lazaro,J.M., Bernad,A., Blasco,M.A., Salas,M. and Blanco,L. (1992) Site-directed mutagenesis at the Exo III motif of phi 29 DNA polymerase; overlapping structural domains for the 3′-5′ exonuclease and strand-displacement activities. *EMBO J.*, **11**, 4227–4237.
57. Thomas,R.K., Nickerson,E., Simons,J.F., Janne,P.A., Tengs,T., Yuza,Y., Garraway,L.A., LaFramboise,T., Lee,J.C., Shah,K. *et al.* (2006) Sensitive mutation detection in heterogeneous cancer specimens by massively parallel picoliter reactor sequencing. *Nat. Med.*, **12**, 852–855.
58. Druley,T.E., Vallania,F.L., Wegner,D.J., Varley,K.E., Knowles,O.L., Bonds,J.A., Robison,S.W., Doniger,S.W., Hamvas,A., Cole,F.S. *et al.* (2009) Quantification of rare allelic variants from pooled genomic DNA. *Nat. Methods*, **6**, 263–265.
59. Bernad,A., Blanco,L., Lazaro,J.M., Martin,G. and Salas,M. (1989) A conserved 3′—-5′ exonuclease active site in prokaryotic and eukaryotic DNA polymerases. *Cell*, **59**, 219–228.
60. Biles,B.D. and Connolly,B.A. (2004) Low-fidelity Pyrococcus furiosus DNA polymerase mutants useful in error-prone PCR. *Nucleic Acids Res.*, **32**, e176.
61. Drake,J.W. and Holland,J.J. (1999) Mutation rates among RNA viruses. *Proc. Natl Acad. Sci. USA*, **96**, 13910–13913.
62. Drake,J.W., Charlesworth,B., Charlesworth,D. and Crow,J.F. (1998) Rates of spontaneous mutation. *Genetics*, **148**, 1667–1686.
63. Schaffer,D.V., Koerber,J.T. and Lim,K.I. (2008) Molecular engineering of viral gene delivery vehicles. *Annu. Rev. Biomed. Eng.*, **10**, 169–194.
64. Stemmer,W.P. (1994) Rapid evolution of a protein in vitro by DNA shuffling. *Nature*, **370**, 389–391.
65. Zhao,H., Giver,L., Shao,Z., Affholter,J.A. and Arnold,F.H. (1998) Molecular evolution by staggered extension process (StEP) in vitro recombination. *Nat. Biotechnol.*, **16**, 258–261.
66. Miura,Y., Yoshida,K., Nishimoto,T., Hatanaka,K., Ohnami,S., Asaka,M., Douglas,J.T., Curiel,D.T., Yoshida,T. and Aoki,K. (2007) Direct selection of targeted adenovirus vectors by random peptide display on the fiber knob. *Gene Ther.*, **14**, 1448–1460.
67. Lupold,S.E., Kudrolli,T.A., Chowdhury,W.H., Wu,P. and Rodriguez,R. (2007) A novel method for generating and screening peptides and libraries displayed on adenovirus fiber. *Nucleic Acids Res.*, **35**, e138.
68. Maheshri,N., Koerber,J.T., Kaspar,B.K. and Schaffer,D.V. (2006) Directed evolution of adeno-associated virus yields enhanced gene delivery vectors. *Nat. Biotechnol.*, **24**, 198–204.
69. Soong,N.W., Nomura,L., Pekrun,K., Reed,M., Sheppard,L., Dawes,G. and Stemmer,W.P. (2000) Molecular breeding of viruses. *Nat. Genet.*, **25**, 436–439.
70. Edfeldt,N.B., Harwood,E.A., Sigurdsson,S.T., Hopkins,P.B. and Reid,B.R. (2004) Solution structure of a nitrous acid induced DNA interstrand cross-link. *Nucleic Acids Res.*, **32**, 2785–2794.
71. Jogler,C., Hoffmann,D., Theegarten,D., Grunwald,T., Uberla,K. and Wildner,O. (2006) Replication properties of human adenovirus in vivo and in cultures of primary cells from different animal species. *J. Virol.*, **80**, 3549–3558.
72. Wong,S.W., Wahl,A.F., Yuan,P.M., Arai,N., Pearson,B.E., Arai,K., Korn,D., Hunkapiller,M.W. and Wang,T.S. (1988) Human DNA polymerase alpha gene expression is cell proliferation dependent and its primary structure is similar to both prokaryotic and eukaryotic replicative DNA polymerases. *EMBO J.*, **7**, 37–47.
73. Delarue,M., Poch,O., Tordo,N., Moras,D. and Argos,P. (1990) An attempt to unify the structure of polymerases. *Protein Eng.*, **3**, 461–467.